

THREE-DIMENSIONAL NUMERICAL EVALUATION OF LIGHTWEIGHT AGGREGATE COMPRESSIVE STRENGTH

**Aldemon L. Bonifácio^{a,1}, Julia C. Mendes^{a,2}, Fernanda M. Cunha^{a,3},
Michele C. R. Farage^{a,4}, Flavio S. Barbosa^{a,5} and Sophie Ortola^b**

^a*Federal University of Juiz de Fora, Brazil, aldemon@ice.ufjf.br¹, julia.mendes@engenharia.ufjf.br²,
fernanda.moreira@engenharia.ufjf.br³, michele.farage@ufjf.edu.br⁴, flavio.barbosa@ufjf.edu.br⁵*

^b*University of Cergy-Pontoise, France, sophie.ortola@u-cergy.fr*

Keywords: Concrete Modeling, Lightweight Aggregates, FEM Analysis, Mechanics of Materials.

Abstract. It is well known that the mechanical behavior of Lightweight Aggregate Concrete (LWAC) is strongly influenced by the Lightweight Aggregate's properties. A number of these properties - such as the LWA's failure strength - are rather difficult to measure experimentally. Taking this fact into consideration, researches has developed analytical procedures in order to identify the LWA's strength through iterative homogenization approaches, showing good agreement with experimental data.

The present work aims to present the results of a numerical program in which the compressive behavior of LWAC's samples was simulated through 3D models using the Finite Element Method. The samples were modeled so as to reproduce an experimental program extracted from in the literature: the material was considered as biphasic, composed of mortar - for which the mechanical properties were experimentally measured - and LWA, for which the properties obtained analytically by Ke et al. (2014) were adopted. Numerical results showed fair agreement with experimental data, encouraging further applications with a higher level of complexity concerning geometrical and mechanical aspects.

1 INTRODUCTION

Lightweight Aggregate Concrete (LWAC) is a versatile material that has been used in civil and naval construction worldwide for decades. Some of its main advantages over Normal-weight Aggregate Concrete (NWAC) are: reduced dead load due to low self-weight, economy in transport and formwork, better thermal and acoustic insulation, and improved fire resistance, which may lead to a reduction in the overall cost of project. The use of LWAC allows for reduced sections on structural elements, larger spans, decreased amount of required steel, and therefore can be economically and efficiently applied to several types of buildings. Although LWAC presents reduced weight and thus a structural advantage, its mechanical resistance is in general lower than that of ordinary concretes. In spite of this, the material is employed in civil construction in structural (load bearing) and non-structural elements. The examples below illustrate its efficiency when applied to high-rises construction. The One Shell Plaza Tower, a 220m office building in Houston, has all its structural elements incorporating lightweight aggregates (Fig. 1). In turn, the Barclays Bank Head Office, located in Canary Wharf, London, is an example of mixed construction technics – its structure is based on steel frame, whereas the slabs are built with composite deck slabs of lightweight aggregate concrete (Fig. 2). In both cases, LWAC was used as a form of reducing the weight of the elements, improving room insulation, besides adding hours of fire resistance with no extra measure, allying economical and safety advantages.



Figure 1: One Shell Plaza Tower, Houston, USA. (Khan, 2004)



Figure 2: Barclays Bank Head Office, London, UK (Lytag, 2013).

Differently from NWACs, where the aggregate is more resistant than the mortar and cracking begins in the interfacial transition zone (ITZ), in LWACs the weakest phase is the aggregate – which has a strong influence on the concrete's properties (Ke *et al.*, 2009). Despite this, stresses inside the aggregates are considerably inferior to the ones inside the mortar, once Young's modulus of the aggregate is, normally, considerably smaller. Due to this characteristic, the rupture mechanism of LWAC is strongly connected to relationships between mortar/aggregate Young's

moduli and also mortar/aggregate compressive strengths. Fig. 3 shows the aspect of expanded clay grains while Fig. 4 illustrates the longitudinal section of a cylindrical sample made of LWAC.

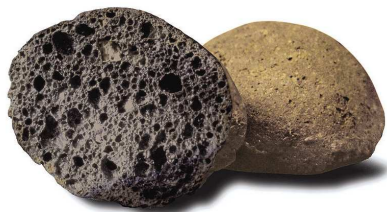


Figure 3: Lightweight Aggregate – Expanded Clay (picture: public domain).

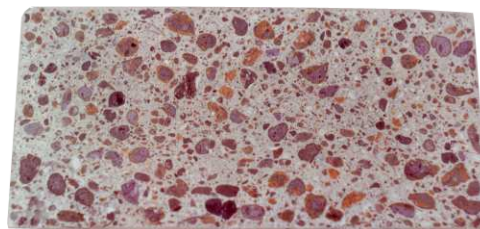


Figure 4: Longitudinal section of a LWAC specimen (GDACE, 2004).

For practical design purposes, it is convenient to be able to estimate the mechanical properties of hardened concrete based on its composition. Concerning LWAC's, though, this is a rather complex task due to the fact that the mechanical properties of LWAs are not precisely measured through experimental techniques. Amongst the methods currently employed to evaluate LWA's compressive strength are experimental procedures and empirical correlations to its bulk density. The standard experimental method is the aggregate crushing test, which records the required pressure for the specimen to reach a 20mm or 50mm compression by means of a hydraulic press (BS EN 13055-1:2003)(British Standards Institute Staff, 2002). The resultant compressive strength of the aggregate from the crush test ($f_{a,exp}$), however, does not accurately reflect the failure mode of the LWA in the concrete (Ke et al., 2014); thus impairing the prediction of the LWAC compressive strength. In turn, empirical equations that relate the compressive strength to bulk densities fail to consider inherent characteristics of the aggregate (i.e. composition, origin, storage conditions, handling) and hence are not considered as reliable options for the material's characterization.

In a previous work, Ke et al. (2014) employed an analytical inverse method for estimating the compressive strength of LWAs (f_a). Through a micromechanical scheme, the authors managed to obtain this property from experimental compressive strengths (f_c) measured on LWAC samples. The adopted input parameters were: Compressive strength (f_m) and Young modulus (E_m) of the mortar matrix (experimentally obtained), volume fraction of LWA adopted in the concrete's mixture, compressive strength measured on hardened LWAC specimens (f_c) and Young modulus of the LWA (E_a), evaluated with Eq. (1):

$$E_a = 8000\rho_{ard}^2 \quad (1)$$

where ρ_{ard}^2 is the dry density of the lightweight aggregate (Ke et al., 2014).

By adopting the aggregate and the mortar properties - f_a , E_a , f_m and E_m - experimentally and/or analytically measured - the present study simulates the behavior of LWAC specimens when subjected to compressive load. To this end, this study employed an Finite Element (FE) open source program, called Cast3M, developed by the French Atomic Energy and Alternative Energies Commission (*Commissariat à L'énergie Atomique et aux Énergies Alternatives*, CEA). The output of the numerical analysis is an estimate of the compressive strength (f_c) of the LWAC. For validation purposes, the numerical data are compared to the results of an experimental program where the $f_{c,exp}$ of LWAC cylindrical specimens was measured via mechanical

tests.

2 NUMERICAL PROGRAM

2.1 Overall Description

The numerical program described herein was accomplished through Cast3M. This software applies the Finite Element Method to several areas, such as elasticity, elastoviscoplasticity problems, among others (Le Fichoux, 2011). Cast3M employs a specific high level object oriented macro-language - Gibiane - where the solver is integrated with pre-processing and post-processing tools. In the present analysis, the LWAC is assumed as a biphasic medium, composed of mortar (m) and LWA (a).

2.2 Reference Experimental Data

Experimental results obtained from a set of LWAC cylindrical samples made of ordinary mortar with 12,5% of expanded clay 4/10 was taken as benchmark for the present work. The material properties adopted for validation purposes in this study were extracted from reference (Ke et al., 2014) and are summed in Table 1. The aggregate gradation is shown in Table 2.

	Descrição	Valor (MPa)
E_a	(LWA's Young's modulus)	8030.00
E_m	(Mortar's Young's modulus)	28600.00
f_a	(LWA's compressive strength)	18.30
f_m	(Mortar's compressive strength)	40.20
p_a	(LWA's tensile strength)	(*) 2.41
p_m	(Mortar's tensile strength)	(**) 8.04
$f_{c,exp}$	(LWAC's compressive strength)	39.00

Table 1: Material's properties (Ke et al., 2014).

(*) This value was obtained from equation (BS EN 13055-1:2002)(British Standards Institute Staff, 2002) $p_a = 3.9(1.82\rho_{av}/1000 - 0.4)$, where ρ_{av} is the bulk density. In the present case, $\rho_{av} = 560\text{kg/m}^3$.

(**) p_m was assumed as 20% of f_m (Rao, 2001).

Sieve Size (mm)	% Cumulative Refusal
12,5	0
10,0	4,68
8,0	67,13
6,3	85,44
5,0	94,84
4,0	97,85
2,5	99,79
1,25	99,94
pan	100

Table 2: Lightweight aggregate gradation.

2.3 3D Finite Element Modeling of the LWAC Specimens

The geometry of the 3D models described in this section represents a 1/8th section of a standard cylindrical sample with 16cm of diameter and 32cm high (Ke et al., 2014), as shown in Fig. 5a. The aggregates are considered as spherical – which is considered an adequate simplifying hypothesis for expanded clay particles, as one can see in Fig. 3. The spheres are randomly distributed and immerse in mortar, here assumed as a homogenous material. The LWA diameter's distribution reproduces the actual aggregate gradation adopted in the mixture, given in the reference work (Ke et al., 2014) and presented in Table 2.

By taking advantage of the symmetry characteristics concerning loading and geometry, Fig. 5 represents the model employed in the present simulations. The boundary conditions were adopted as follows (see Fig. 5b): section ABCD is restrained in the Y direction; section AEFD, in restrained in the X direction and section ABE, in the Z direction. These boundary conditions were adopted so as to reproduce a compressive test, and the schematic loading is indicated in Fig. 5b.

In order to account for the dispersion of results, thirty 3D models were generated from the same synthetic sample, each one presenting a different random spatial aggregate distribution.

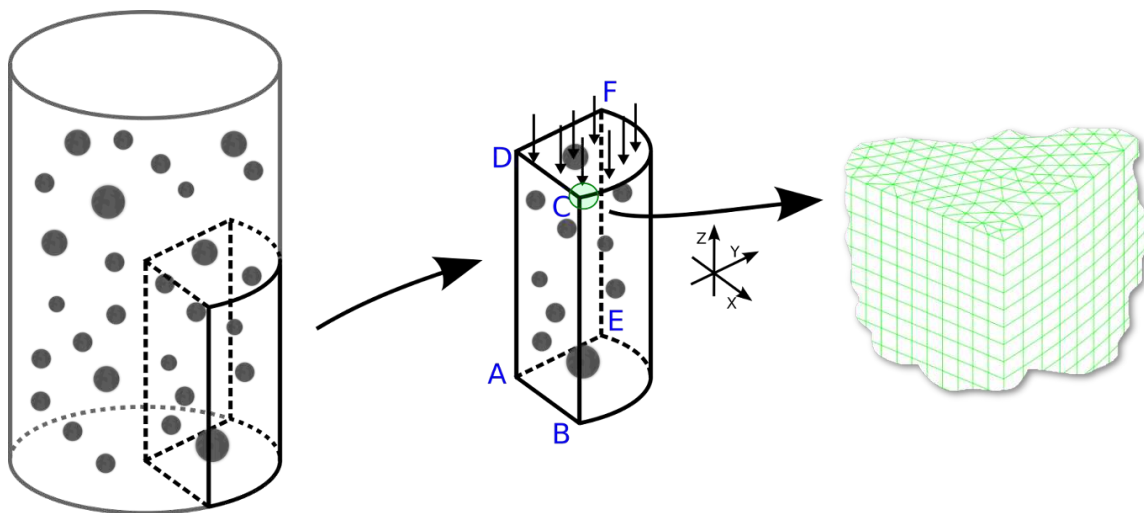


Figure 5: Numerical representation of a LWAC sample: (a) geometry of the numerical sample showing the concrete and aggregates in gray; (b) geometrical model employed in the numerical simulations so as to represent 1/8th of a LWAC cylinder; (c) Typical FE mesh with six-noded wedge elements.

2.4 Failure Analysis

E_a , f_a , E_m and f_m (from Table 1) are the input mechanical parameters for the numerical analysis, which consisted of subjecting the modeled concrete specimens to incremental compressive loads (as indicated in Fig. 5c) up to failure.

The compression stress level of a finite element is defined by means of a quantity named *compression stress level* ($c_\alpha(i)$) where the α index indicates the phase of the i -th finite element: m for mortar and a for LWA. The $c_\alpha(i)$ coefficient is evaluated according to Eq. (2):

$$c_\alpha(i) = \frac{\text{abs}(\sigma_3(i))}{f_\alpha} \quad (2)$$

where $\sigma_3(i)$ is the maximal compressive stress observed in the i -th element and f_α is the phase's compressive strength (see Table 1).

The *tensile stress level* ($t_\alpha(i)$) is evaluated for every finite element in an analogous manner, as given in Eq. (3):

$$t_\alpha(i) = \frac{\sigma_1(i)}{p_\alpha} \quad (3)$$

where $\sigma_1(i)$ is the maximal tensile stress in the i -th finite element and p_α is the phase's tensile strength (given in Table 1).

The i -th element is considered to reach failure - either under compression or tension - when $c_\alpha(i)$ and/or $t_\alpha(i)$ are ≥ 1 .

It is possible to identify the global failure of a LWAC specimen when a significant amount of finite elements reaches failure. The main goal of the adopted computational procedure is to verify whether the resulting compressive strength numerically obtained approaches its experimental counterpart, $f_{c,exp} = 39\text{MPa}$ (given in Table 1).

3 NUMERICAL RESULTS

This work consists of a linear elastic analysis. In spite of this fact, the adopted approach showed fair agreement with the reference measurements, as one can see in the following.

In order to verify the convergence of the numerical results, 7 different meshes with increasing refinement levels were adopted to model the 3D concrete sample under longitudinal loading of 15MPa: M1 (2,520 elements); M2 (20,880 elements); M3 (71,280 elements); M4 (169,440 elements); M5 (332,800 elements); M6 (574,320 elements) and M7 (915,880 elements). Fig. 6 illustrates the results obtained for the vertical displacement (δ) on the top of the specimen for each adopted mesh (M_i) related to that evaluated for mesh M7. As one can see in the figure, results are almost coincident for meshes M5, M6 and M7. Based on this consideration, mesh M5 was adopted for the present analysis, having an amount of 527,220 degrees of freedom.

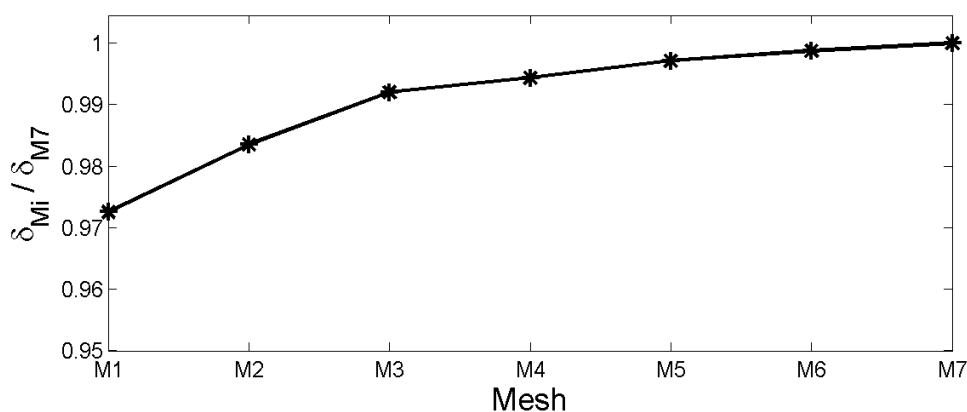


Figure 6: Convergence analysis: the curve represents the variation of the vertical displacement on the top of the numerical model for seven different FE meshes.

Fig. 7 to Fig. 10 show typical results in terms of compression stress level (c_α) and tensile stress level (t_α) for a loading of 10MPa.

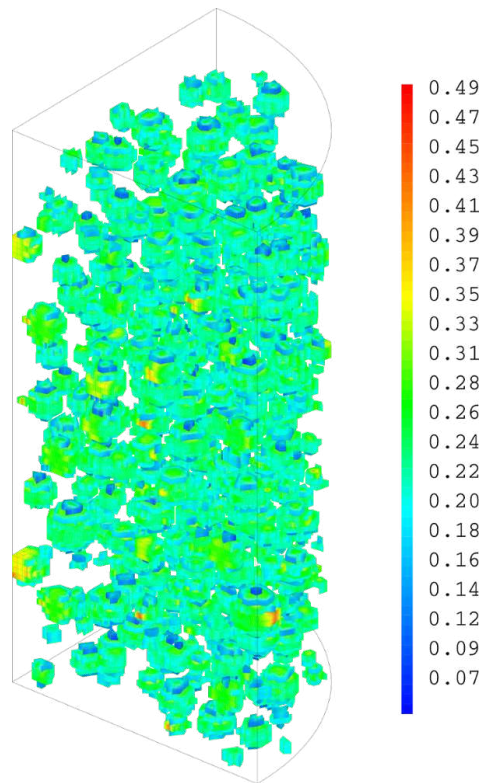


Figure 7: c_a distribution for finite elements modeling aggregates.
Scale indicates c_a level (Eq. (2)).

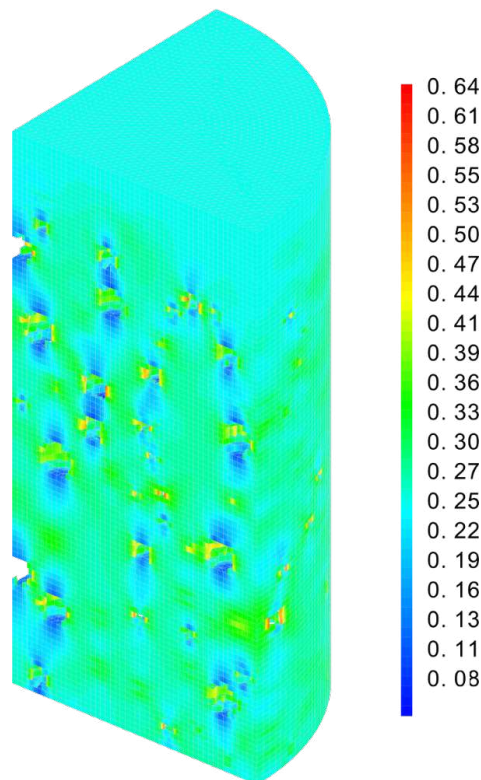


Figure 8: c_m distribution for finite elements modeling mortar.
Scale indicates c_m level (Eq. (2)).

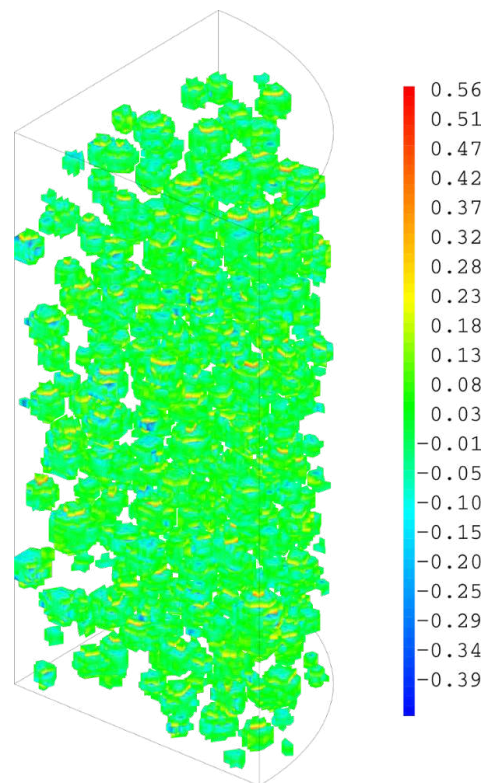


Figure 9: t_a distribution for finite elements modeling aggregates.
Scale indicates t_a level (Eq. (3)).

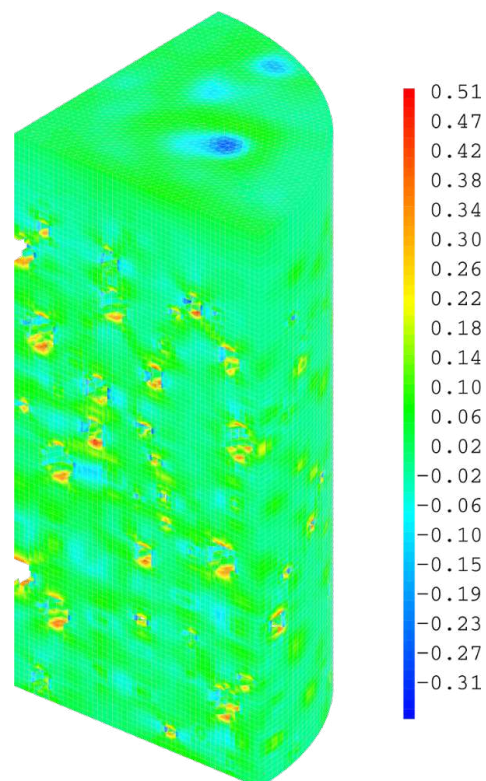


Figure 10: t_m distribution for finite elements modeling mortar.
Scale indicates t_m level (Eq. (3)).

Fig. 11 to Fig. 14 show the amount of failed elements resulting from applied compressive stresses varying from 25MPa to 39MPa. The boxplots presented in such figures result from the 30 analyses performed on the numerical specimens, as mentioned in Section 2.3 - the red lines standing for the median values.

Fig. 11 and Fig. 13 demonstrates the evolution of the amount of finite elements made of LWA (a_{FE}) under compressive or tensile failure, respectively. It is possible to observe that, practically, there were not failure elements for all levels of applied loads.

Fig. 12 and Fig. 14 are related to the finite elements composed of mortar (m_{FE}). It is seen in Fig. 12 that the amount of m_{FE} reaching compressive failure varies from 10% - for a 33MPa loading - to around 70% under 39MPa. On the other hand, Fig. 14 shows that there was practically no m_{FE} under tensile failure ($c_m \geq 1$) for the applied load levels, except for 39MPa.

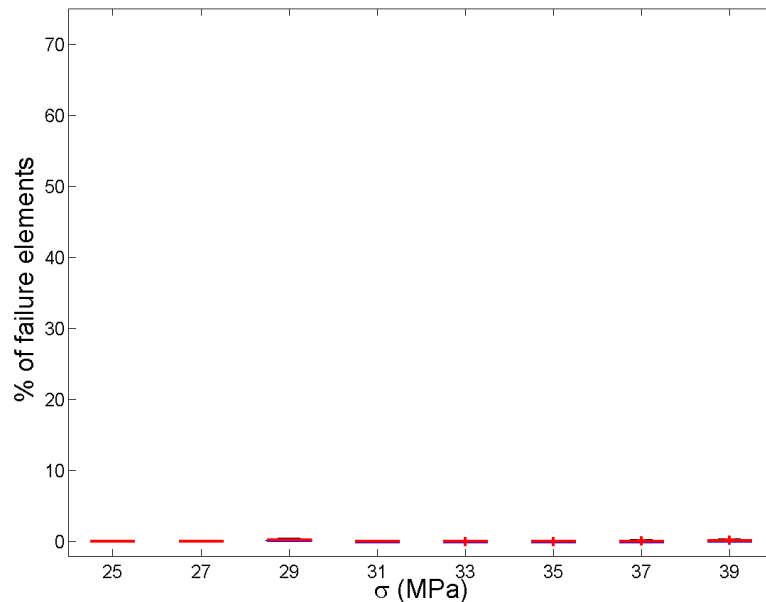


Figure 11: Evolution of the amount of aggregate - a_{FE} - under compressive failure ($c_\alpha \geq 1$).

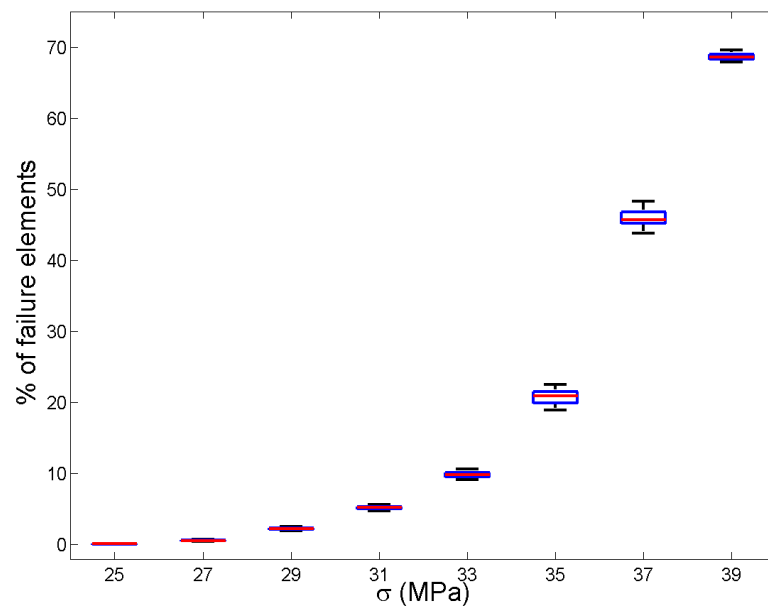


Figure 12: Evolution of the amount of mortar - m_{FE} - under compressive failure ($c_m \geq 1$).

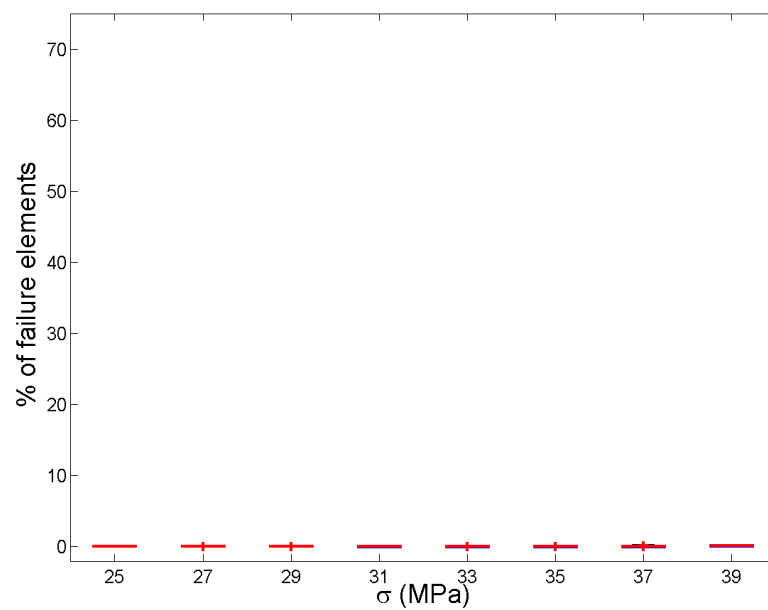


Figure 13: Evolution of the amount of aggregate - a_{FE} - under tensile failure ($t_a \geq 1$).

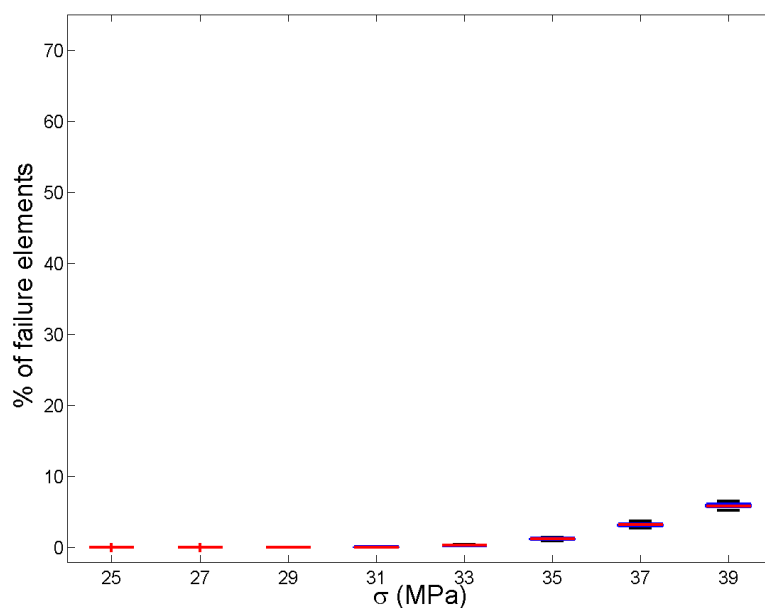


Figure 14: Evolution of the amount of mortar - m_{FE} - under tensile failure ($t_m \geq 1$).

4 DISCUSSION

In the present analysis, the LWAC sample is considered to reach global failure when a significant amount of finite elements reach their respective stress limits (c_α and/or $t_\alpha \geq 1$). Fig. 12 to Fig. 14 indicate that such a situation is not observed for loadings up to 33MPa. From that stage on, an increasing number of finite elements attain failure at each loading step. As the amount of elements under failure is around 10% for the 33MPa loading and more than 70% for 39MPa (see Figs. 11 to 14), the numerical result for the LWAC's compressive strength, though, is estimated as ranging from 33MPa to 39MPa. Such a result is considered to fairly agree with the experimental benchmark, of 39MPa.

It is important to notice that the present study does not take into account some specific phenomena that influence the material's macroscopic behavior. For instance, the linear mechanical model adopted herein for both the concrete's components does not reproduce any stress redistribution resulting from localized failure. This aspect shall be improved by assuming an elastoplastic non-linear mechanical model, which is expected to increase the global material's strength.

This work is the starting stage of a comprehensive study aiming to apply computational modeling allied to experimental data to the better understanding and prediction of LWAC's behavior. In spite of the simplifying hypothesis adopted in this stage of the work, the numerical results obtained herein showed fair agreement with their experimental counterpart. This fact encourages further applications with higher complexity related to geometric and mechanical aspects, in order to better reproduce and preview real world problems.

It is important to notice that, for the present case, the relationship between mortar/aggregate Young's moduli is, approximately, 3.5 and relationship between mortar/aggregate compressive strength is close to 2. These ratios indicate that, for a same strain level, the mortar develops stresses around 3.5 times higher than the ones in the aggregate. In that way, even having a

compressive strength twice bigger, the failure mechanism is expect to start in the mortar. This expectation also could be observed in the numerical tests.

ACKNOWLEDGEMENTS

Authors would like to thank: CNPq (Conselho Nacional de Desenvolvimento Científico e Tecnológico); UFJF (Federal University of Juiz de Fora); FAPEMIG (Fundação de Amparo à Pesquisa do Estado de Minas Gerais) and CAPES (Coordenação de Aperfeiçoamento de Pessoal de Nível Superior) for financial supports.

REFERENCES

- British Standards Institute Staff. *Lightweight Aggregates. Lightweight Aggregates for Concrete, Mortar and Grout*. B S I Standards, 2002. ISBN 9780580397769.
- GDACE. Grupo de desenvolvimento e análise do concreto estrutural. <http://www.gdace.uem.br/linhas.htm>, 2004. Accessed: 2014-03-12.
- Ke Y., Beaucour A., Ortola S., Dumontet H., and Cabrillac R. Influence of volume fraction and characteristics of lightweight aggregates on the mechanical properties of concrete. *Construction and Building Materials*, 23(8):2821–2828, 2009.
- Ke Y., Ortola S., Beaucour A., and Dumontet H. Micro-stress analysis and identification of lightweight aggregate's failure strength by micromechanical modeling. *Mechanics of Materials*, 68:176–192, 2014.
- Khan Y.S. *Engineering architecture: the vision of Fazlur R. Khan*. WW Norton & Company, 2004.
- Le Fichoux E. *Présentation et utilisation de CASTEM*. CEA, 2011.
- Lytag. Project profile - structural – Barclays Bank, Canary Wharf. <http://www.lytag.net/uploads/projects/files/Structural%20%20Barclays%20Bank.pdf>, 2013. Accessed: 2014-03-12.
- Rao G.A. Generalization of abrams' law for cement mortars. *Cement and Concrete Research*, 31(3):495–502, 2001.